Brain Stimulation 18 (2025) 1620–1631

Contents lists available at ScienceDirect

Brain Stimulation

journal homepage: www.journals.elsevier.com/brain-stimulation

Effects of atorvastatin-loaded PEGylated liposomes delivered by magnetic stimulation for stroke treatment

Ji-Hye Kim [a,1], Ja-Hae Kim [b,1], Hafiz Ashfaq Ahmad [c,1], Hohyeon Kim [c], Raveena Nagareddy [d], Kang-Ho Choi [a,d,*], Jungwon Yoon [c,**], Yong-Yeon Jeong [e,***]

[a] Department of Neurology, Chonnam National University Medical School and Hospital, Gwangju, South Korea
[b] Department of Nuclear Medicine, Chonnam National University Medical School and Hospital, Gwangju, South Korea
[c] School of Integrated Technology, Gwangju Institute of Science and Technology, Gwangju, South Korea
[d] Department of Biomedical Sciences, Chonnam National University Medical School and Hwasun Hospital, Hwasun, South Korea
[e] Department of Radiology, Chonnam National University Medical School and Hwasun Hospital, Hwasun, South Korea

ARTICLE INFO

Keywords:
BBB
Delivery
Ischemic stroke
LipoStatin
Magnetic stimulation
Nanoparticle

ABSTRACT

Background: Focused magnetic stimulation (MagStim) can temporarily and safely open the blood-brain barrier (BBB) for target delivery. We investigated whether opening the BBB with MagStim and delivering atorvastatin-loaded PEGylated liposomes (LipoStatin) would work synergistically for subacute post-stroke treatment.
Methods: Two weeks after middle cerebral artery occlusion (MCAO), an injection of 15 mg/ml magnetic nanoparticles (MNPs) was performed, followed by 30 min of MagStim, in subacute stroke models. The procedure was conducted over a week, during which MagStim and MNPs were administered three times at two-day intervals, and LipoStatin (10 mg/kg) was injected immediately after each MagStim treatment. We investigated the motor function, BBB integrity, neuroinflammation, and neurogenesis three weeks after stroke (Sham vs. Control vs. LipoStatin vs. MagStim + LipoStatin).
Results: The MagStim + LipoStatin group showed improved motor function compared to the Control ($p = 0.007$) group. The MagStim + LipoStatin group significantly reduced infarct volume and improved BBB integrity compared to the control and LipoStatin groups. In the MagStim + LipoStatin group, the expression of TNF-α was reduced ($p = 0.020$) compared to the LipoStatin group, and eNOS was enhanced ($p = 0.037$) compared to the Control group. Markers for neurogenesis were also considerably increased in the MagStim + LipoStatin group compared to the Control and LipoStatin groups ($p < 0.0001$).
Conclusions: Our study demonstrates the beneficial synergistic effects of MagStim and the target delivery of LipoStatin in subacute ischemic stroke. These findings underscore the need for future advancements in promising novel non-invasive MagStim methods and nanotherapeutic hybrid approaches for target drug delivery and treatment in post-stroke recovery.

1. Introduction

Ischemic stroke is the leading cause of death and disability, impairing brain function to varying degrees [1]. Recovery from stroke-related disability is a desired and necessary aspect of stroke research. Thus, different treatments have been proposed to alleviate stroke-induced brain damage and restore motor function [2–4]. Endovascular thrombectomy (EVT) is currently the standard of care for large vessel occlusion (LVO) of acute stroke patients [5]. However, despite the high rate of successful reperfusion after EVT, the proportion of poor functional outcomes with dependence is more than half in patients treated with EVT [6]. Treatment options that can restore brain function in subacute

* Corresponding author. Department of Neurology, Chonnam National University Medical School and Hospital 42 Jebongro, Donggu, Gwangju, 61469, South Korea.
** Corresponding author.
*** Corresponding author. Department of Radiology, Chonnam National University Medical School and Hwasun Hospital, 322 Seoyang-Ro, Hwasun-Eup, Hwasun-Gun, Jeollanam-Do, 58128, South Korea.
E-mail addresses: ckhchoikang@chonnam.ac.kr (K.-H. Choi), jyoon@gist.ac.kr (J. Yoon), yjeong@jnu.ac.kr (Y.-Y. Jeong).
[1] These authors contributed equally to the manuscript.

https://doi.org/10.1016/j.brs.2025.08.024
Received 7 May 2025; Received in revised form 20 August 2025; Accepted 28 August 2025
Available online 29 August 2025

to chronic stroke after acute reperfusion therapy remain limited [7]. There is no specific treatment option other than secondary prevention and rehabilitation [7]. Therefore, safely targeting therapy of a potentially neuroprotective agent to the damaged areas in a non-invasive manner to minimize neurological deficits is one of the most essential residual unmet needs among patients with a functional disability after stroke. In addition, drug delivery to target brain regions of therapeutic agents is a challenge that needs to be addressed because it is limited by the protective barrier of the blood-brain barrier (BBB).

Statins, technically called 3-hydroxy-3-methylglutaryl coenzyme A reductase inhibitors, are used to treat individuals with ischemic stroke or vascular disease [8]. Statins effectively improve endothelial function, decrease inflammation, and act as neuroprotective antioxidants by inhibiting NADPH oxidase-derived superoxide [9,10]. Previously, we used atorvastatin-loaded PEGylated liposomes (LipoStatin) in an acute stroke model, demonstrating the effective delivery of LipoStatin to ischemic brain lesions. Additionally, LipoStatin showed significant neuroprotective effects and promoted functional recovery by enhancing endothelial function and inhibiting inflammation.

Recent studies have shown that nanoparticle (NP)-based targeting and delivery are promising not only for the early and accurate identification of stroke risk but also for effective treatment of acute ischemic stroke [11]. However, the critical determinant of treatment effectiveness in subacute-to-chronic ischemic stroke is influential drug delivery to the brain through the blood-brain barrier (BBB). Delivering drugs to the brain through non-invasive stimulation has recently been attempted. In this approach, focused nanomagnetic brain stimulation (MagStim) is an innovative technology that can effectively deliver drugs to the brain through non-invasive brain stimulation [12,13]. We have recently demonstrated that focused magnetic heating can deliver drugs by stimulating target areas to overcome the BBB in subacute-to-chronic stroke while minimizing side effects [14]. Additionally, we previously confirmed the efficacy of LipoStatin in acute ischemic stroke [15].

Thus, this study aimed to investigate whether overcoming the BBB with MagStim and delivering therapeutic agents of LipoStatin to target ischemic areas could effectively and safely treat subacute stroke following acute reperfusion (Fig. 1).

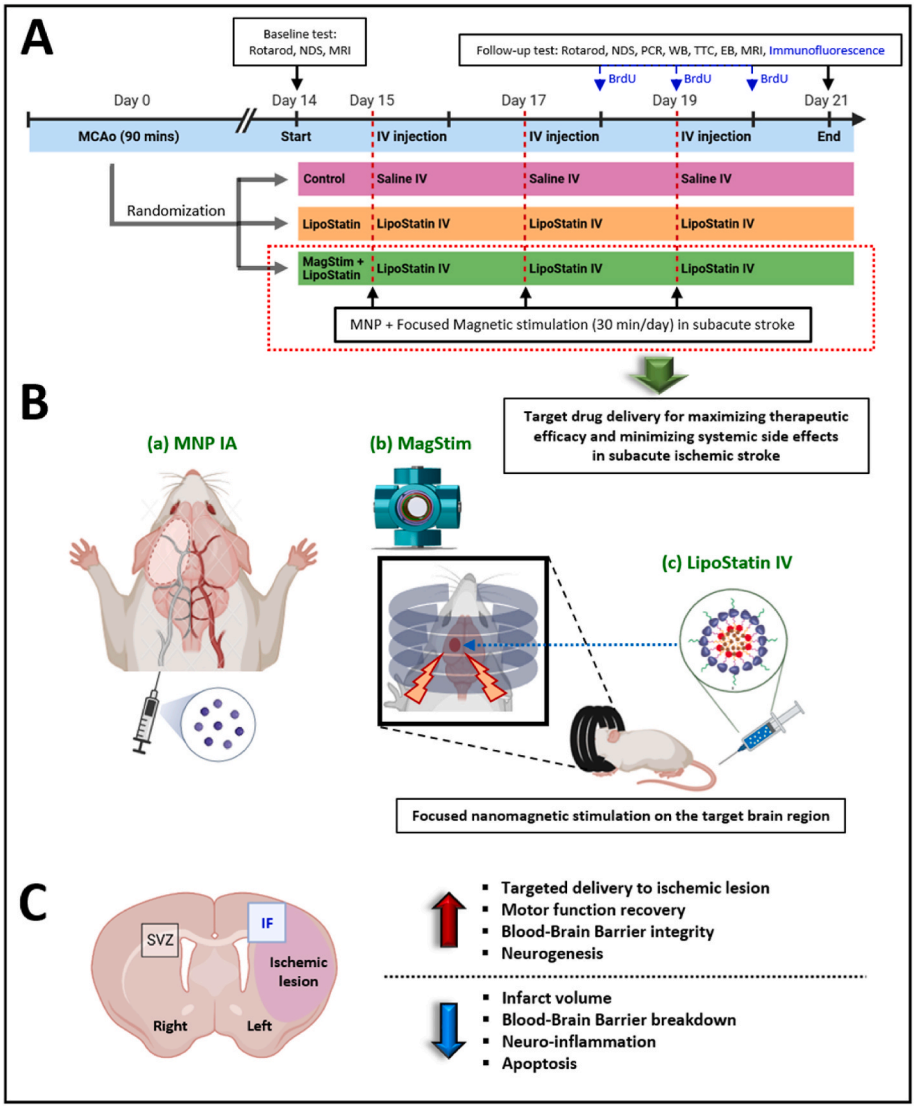

Fig. 1. Experimental arrangement. (A) Magnetic nanoparticles (MNPs, 15 mg/ml) were injected via the carotid artery. For one week, magnetic stimulation was applied to the target brain area thrice at 2-day intervals, each session lasting 30 min per day. (B) The magnetic stimulation was focused on the target brain region of the ischemic hemisphere for drug delivery. (C) Immunofluorescence (IF) staining was conducted in the boundary area adjacent to the subventricular zone (SVZ) of the frontal cortex.

2. Materials and methods

2.1. Ethics statement and data availability

The Institutional Animal Care and Use Committee (IACUC) approved all procedures involving animals, and the guidelines for the ethical care and use of laboratory animals at Chonnam National University were followed (CNUHIACUC-22033). The experimental procedures were based on the guidelines for the ethical care and use of animals in research provided by the National Institutes of Health (NIH, Bethesda, MD, USA). All supporting data within the article can be obtained from the corresponding author upon reasonable request from a qualified investigator.

2.2. Animals and surgical procedures

Animals had free access to food and water and no behavioral restrictions. Adult (8-week-old) male Sprague-Dawley (SD) rats weighing 250–290 g were purchased from Samtako Bio Korea Co., Ltd. (Seoul, Korea). As previously described, the MCA occlusion (MCAO) model was induced using the intraluminal filament technique and reperfused for 90 min in SD rats to simulate the situation in patients receiving reperfusion therapy of EVT for acute LVO [16]. Each animal was anesthetized with isoflurane (3 % for induction, 2 % for maintenance) in a mixture of oxygen/nitrous oxide (30 %/70 %) administered via a mask. The rats' body temperature was maintained at 36.6 ± 0.5 °C during and after the surgery using a temperature-controlled heating pad. All efforts were made to minimize pain during anesthesia. Two weeks after MCAO, 15 mg/mL magnetic NP (MNP) was intra-arterial (IA) delivered via the internal carotid artery (ICA), followed by 30 min of magnetic stimulation in the rat brain. Magnetic stimulation and MNP injections were performed thrice at 2-day intervals for 1 week. The sample size for each experiment was chosen empirically to provide adequate statistical power to detect a treatment effect. The animals were randomly assigned to four treatment groups (n = 6 per group/experiment), and the investigators who assessed the outcomes were blinded to group assignment (Fig. 1A). In the first experimental group, normal rats underwent sham surgery without MCAO (Sham group). In the second experimental group, MCAO rats were injected with saline (Control group). MCAO rats were injected with LipoStatin (LipoStatin group) in the third experimental group. In the fourth experimental group, after MNP administration, MCAO rats were subjected to magnetic stimulation for 30 min and then immediately injected with LipoStatin (MagStim + LipoStatin group). Considering the possibility of residual or leaking solution in the syringe during injection, 10 mg/kg of LipoStatin was intravenously injected via the tail vein based on previous studies and our prior dose optimization findings [15,17–19].

2.3. Synthesis of LipoStatin

As previously reported, liposomes were prepared using the film hydration method [15]. Briefly, 1,2-distearoyl-sn-glycero-3-phosphoethanolamine (DSPE-PEG), dipalmitoyl-phosphatidyl-choline (DPPC), and cholesterol were mixed in a ratio of 1.5:1.5:1 (by weight) in each solvent (methanol for DSPE-PEG and DPPC, chloroform for cholesterol). The mixture was then shaken in a glass vial for 2 min. The above solvents evaporated at room temperature to form a thin film in a vacuum chamber. Then, the film was hydrated with 1 ml of distilled water and heated in a glass vial at 60 °C for 30 min to produce multivesicular liposomes with heterogeneous properties. Finally, the LipoStatin NP dispersion was prepared using a probe sonicator (Q125 Sonicator, Qsonica, Newtown, CT, USA) for 10 min (amplitude 20 %, 20 kHz).

2.4. Focused nanomagnetic stimulation

Two disc-shaped permanent magnets were positioned face-to-face with a separation distance of 15.3 cm, and a 17-turn coil with a diameter of 5 cm was placed concentrically between them (Fig. 1B). This configuration generated a magnetic field-free point (FFP) at the center of the setup, where only an alternating magnetic field (AC field) was present. The AC field was generated using a driving current set to 7 mTrms at a frequency of 595.4 kHz. The AC magnetic fields applied in our study operate in the radiofrequency range with long wavelengths and thus were safe without interaction with biological tissues [20]. The animal's head was secured within this FFP using a custom-designed conical head holder to precisely target the brain region associated with the cerebral infarct lesion [21,22].

As used in previous experiments, magnetic nanoparticles (15 mg/mL) were used to open the BBB while ensuring safe stimulation [14]. The localized exposure of these particles to the net AC magnetic field at the FFP induced magnetic relaxation, leading to controlled heating at the highly localized target site, avoiding off-target thermal damage or systemic side effects. A temperature rise of approximately 5 °C was observed at the lesion, within the established safety threshold for rat brain stimulation (39°C-44 °C) [23]. Drug delivery to the target brain region, the cerebral infarction lesion, was achieved through three stimulation treatments every other day.

2.5. Evans Blue staining and fluorescence imaging

BBB permeability changes were assessed using Evans Blue staining. Evans Blue (4 %) was injected into the tail vein and circulated for 2 h. Saline was perfused intracardially to remove blood and Evans Blue dye from the vessels. After euthanasia, brains were extracted, and fluorescence analysis for Evans Blue staining was performed. Extracted brains were sectioned into 2 mm coronal sections, while vascular permeability was assessed by quantifying the extravasation of Evans Blue into the brain using an *in vivo* imaging system (IVIS® Lumina S5, PerkinElmer). Images of the whole brain and 2 mm tissue slices were acquired ex vivo using the following parameters: excitation filter of 600 nm, emission filter of 710 nm, exposure time of 1 s, binning of 8, f-stop of 2, and field of view of 21 cm. Evans Blue fluorescence was observed to analyze regions of interest in the whole brain and slices.

2.6. MPI image of MNP accumulation at the target region

Nanoparticle accumulation in the target region was analyzed using magnetic particle imaging (MPI). Quantification based on MPI images was validated with an error margin of 4.3 ± 1.8 % using samples with known particle mass. Each MPI input signal was normalized, and the volume of slices exceeding a defined brightness threshold was extracted to calculate the total signal brightness. Particle mass was then estimated using a mass estimation factor, defined as the ratio of mass standard deviation to net signal standard deviation.

2.7. Behavioral tests of ischemic stroke model rats

Neurological assessments were performed before treatment and at 1 week post-treatment. The neurological deficit score (NDS) was assessed by an investigator who was unaware of the experimental group. We included only rats with a pretreatment NDS score of 1 or higher. A higher NDS indicated a more severe neurological impairment [24]. Motor dysfunction was assessed using an accelerating rotarod test. Three 5-min activity training sessions were performed for each experimental group before the assessment. Afterward, the rotating drum was accelerated for 5 min, and the time (in seconds) it took for the animals to fall off the drum was recorded before treatment and at 1 week post-treatment. Each session was performed three consecutive times for a maximum of 300 s. The average latency to fall from the three trials was then calculated.

2.8. T2-weighted MR imaging

T2-weighted magnetic resonance (MR) imaging was performed using the M7™ Compact MRI system (Aspect Imaging, Shoham, Israel) to measure the size of the cerebral infarction in the three MCAO groups. Rats were anesthetized using isoflurane (Forane soln. Abbot, USA). The protocol for T2-weighted fast spin-echo MR imaging was as follows: TR/TE 4000/100 ms, TI 100 ms, echo train length 12, flip angle 150°, field of view 4 cm, number of slices 20, slice thickness 1.5 mm, interslice gap 0 mm, matrix 256 × 210. *In vivo* brain MR images were acquired twice (before and 1 week after treatment) in the same rats (n = 6 per group). In T2-weighted MR images, the volume of the infarct area showing high signal intensity was quantified using medical image processing, analysis, and visualization software (MIPAV, NIH, version 8.0.2).

2.9. Determination of infarct volume

Four groups were euthanized after isoflurane anesthesia. The brains were carefully extracted from the skull and sliced coronally at 2-mm intervals starting 1 mm distal to the frontal pole using a rat brain matrix (RBM-4000C; ASI Instruments, Warrin, MI, USA). Coronal sections were stained in phosphate-buffered saline (PBS) containing 2 % 2,3,5-triphenyl tetrazolium chloride (TTC; Sigma) at 37 °C for 10 min [2]. The extent of brain damage over the entire ipsilateral hemisphere was quantified using ImageJ software. Total infarct volume (mm3) was determined by summing the volume of the damaged area in the brain sections (i.e., damaged area × thickness).

2.10. Immunoblot analysis and reverse-transcription polymerase chain reaction

The rats' brains subjected to MCAO were cut in half to separate the left (ischemic) hemispheres (n = 6 for each group). Protein extracts were prepared from the tissues to analyze protein concentration patterns in the ischemic hemisphere. The protein level of caveolin-1 (Cav-1), claudin-5, JAM-A (#ab2910, #ab15106, #ab52647; Abcam, Cambridge, UK), endothelial nitric oxide synthase (eNOS; #32027S; cell signaling technology, Danvers, Massachusetts, USA), MMP-9, occludin, zona occuldens-1 (#MA5-32705, #75–1500, #61–7300; Thermo Scientific, Rockford, IL, USA), Interieukin-1 beta, Interieukin-6, TNF alpha, Iba1 (#12703S, #12912S, #11948S, #17198S; cell signaling technology, Danvers, Massachusetts, USA), and β-actin (#SC-47778; Santa Cruz Biotechnology, Santa Cruz, CA, USA) was investigated. The expression levels were quantified by calculating the mean gray value for each band with ImageJ software.

Total RNA was extracted from the brain, followed by cDNA synthesis. Reverse-transcription polymerase chain reaction (RT-PCR) was performed for tumor necrosis factor-alpha (TNF-α), ionized calcium-binding adaptor molecule 1 (Iba-1), interleukin 1β (IL-1β), IL-6, monocyte chemoattractant protein-1 (MCP-1), eNOS, SRY-box transcription factor 2 (Sox2), and Nestin. Glyceraldehyde-3-phosphate dehydrogenase (GAPDH) was used as an internal control.

2.11. BrdU administration and immunofluorescence

Proliferating cells were labeled with the thymidine analog 5-bromo-2′-deoxyuridine (BrdU; Sigma-Aldrich, St Louis, MO, USA). Each group received an intraperitoneal injection of 50 mg/kg (10 mg/mL), resulting in a solution. For the last three days, BrdU was administered to enhance the labeling of cells that were actively dividing. We conducted double labeling using fluorescent-tagged secondary antibodies to assess neurogenesis. Following a wash with a buffer solution (TBS and 0.1 % Tween 20), we incubated the sections with specific primary antibodies. Antibodies against doublecortin (DCX, #48–1200; Thermo Scientific, Rockford, IL, USA; 1:100) were used for neuronal progenitor cells, NeuN (#ABN78; EMD Millipore, USA; 1:100) was used for mature neurons, and cleaved caspase-3 (CC3, #43–7800; Abcam, USA; 1:100) served as an apoptosis marker. The optical fractionator method was employed to quantify cells exhibiting dual labeling (BrdU/NeuN-positive, BrdU/DCX-positive, or CC3/NeuN-positive cells). Double-labeled cells were enumerated along the boundary region of the frontal cortex adjacent to the subventricular zone in each brain (Fig. 1C).

2.12. Statistical analysis

The normality of data distribution was evaluated using the Shapiro-Wilk test, and Levene's test assessed the homogeneity of variance between groups. Parametric data were analyzed using one-way ANOVA with Tukey's multiple comparison tests and presented as mean ± standard deviation or standard error of the mean. Data with unequal variances were analyzed using ANOVA with Welch's correction, followed by Dunnett's multiple comparisons. Nonparametric data were analyzed using the Kruskal-Wallis test and were presented as median [interquartile range]. The behavior and brain imaging test, involving repeated trials, was assessed for sphericity using Mauchly's test. When the sphericity assumption was violated, Greenhouse-Geisser estimates were used to correct it. After confirming the assumption of equality of covariance between the groups, the test data were analyzed using repeated-measures ANOVA to determine the interaction effect between treatment and time (treatment × time) and the main effects of experimental treatment and time. * indicates $p < 0.05$, ** indicates $p < 0.01$, *** indicates $p < 0.001$ and **** indicates $p < 0.0001$. All measurements were performed by observers blinded to the individual treatments.

3. Results

3.1. Evans Blue staining and fluorescence imaging

We conducted fluorescence imaging analysis using Evans blue to determine when the permeability of the BBB normalized. We analyzed fluorescence imaging with Evans blue on days 1, 3, 7, and 14 after MCAO to evaluate whether the BBB normalized compared to the sham model. We observed that BBB breakdown peaked up to day 3 after MCAO, followed by a decrease from day 7 to day 14. On day 14, the results were similar to those in the non-stroke group (sham). Thus, the BBB disruption caused by ischemic stroke returns to normal levels at 14 days after acute ischemic stroke due to MCAO, diminishing the BBB penetration by LipoStatin (Fig. 2).

3.2. MPI image of MNP accumulation at the target region

Focused heating is generated by the superposition of field-free points induced by a gradient and alternating magnetic fields. Accumulation via the gradient magnetic field was simulated under the following conditions: vessel diameter of 320 μm, flow rate of 25 cm/s, fluid type as blood, gradient field of 2.1 T/m, and particle diameter of 50 nm (Fig. 3A) [22]. We investigated whether target drug delivery by increasing BBB permeability was possible with 15 mg/mL MNP, a lower concentration than 30 mg/mL previously used for BBB opening, since BBB integrity may not be intact in subacute stroke rats. First, the temperature was raised by 5.5 °C through MagStim in normal rats. However, the change in BBB permeability due to this stimulation was not different between the control and experimental groups, as shown by Evans Blue leakage images captured using an IVIS® imaging system (Fig. 3B). Therefore, these results show that target drug delivery is difficult with 15 mg/mL MNP in normal or chronic stroke rats with intact BBB, as in our previous study [14,22].

Next, to evaluate the possibility of target drug delivery and monitoring with 15 mg/mL MNP in the subacute stroke model used in this experiment, MPI was used to estimate the MNP concentration changes in the target brain region after MNP injection at 24, 48, and 72 h. At each

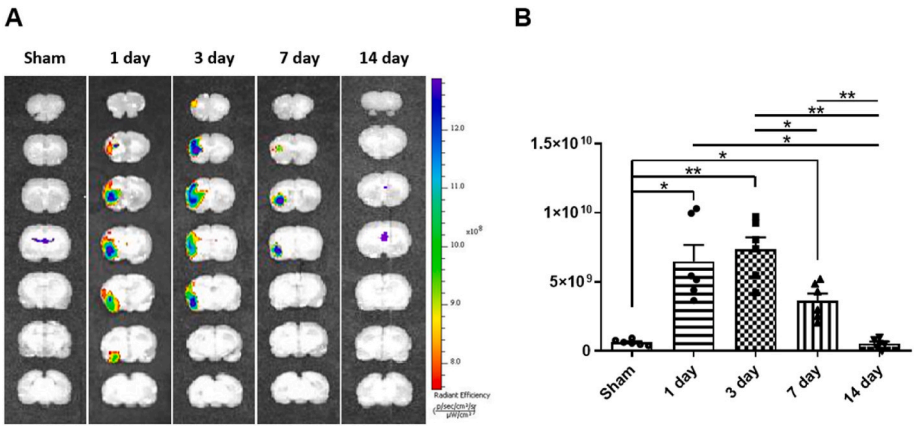

Fig. 2. Evans blue staining and fluorescence imaging. Measurement of Evans blue extravasation up to 14 days after MCAO using a fluorescence imaging system. BBB opening was peaking on day 3 after MCAO. The BBB disruption returned to normal levels 14 days after acute ischemic stroke due to MCAO. Data are presented as mean ± SEM. Data were analyzed by ANOVA with Welch's correction (n = 6). *: $p < 0.05$, **: $p < 0.01$.

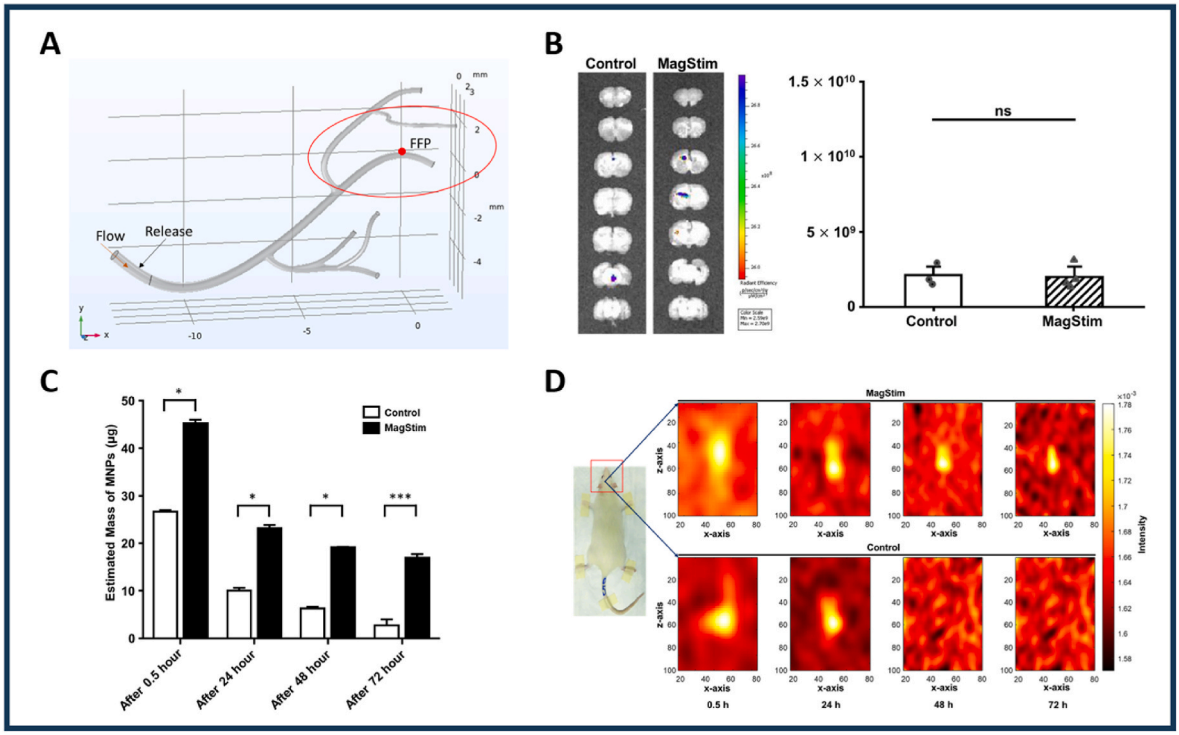

Fig. 3. Change of BBB permeability and MPI image of MNP accumulation at the target brain region. (A) MNP accumulation by the gradient field at the target region was simulated using COMSOL software. (B) Measurement of Evans blue extravasation using a fluorescence imaging system for the Control and MagStim group. (C) Estimated mass of accumulated MNP of each group from the MPI image. (D) 2D MPI image of accumulated MNP at the target brain region for the Control and MagStim groups. Data are presented as the mean ± SD. n = 3 in each group. *: $p < 0.05$, **: $p < 0.01$, ***: $p < 0.001$.

time point, the residual particle concentration in the MagStim group was significantly higher than that in the control group (Fig. 3C). In particular, as shown in the MPI images in Fig. 3D, a high particle residual amount was observed in the target brain region up to 72 h after MagStim administration, with an estimated concentration of at least 16.94 μg, unlike the control group. These results suggest that our drug delivery method of 15 mg/mL MNP injection every other day with MagStim can effectively deliver drugs to targeted regions.

3.3. Characterization of LipoStatin formulation

The quality evaluation results of the LipoStatin were shown in Fig. 4. LipoStatin exhibited a hydrodynamic size of 293 nm, and its zeta potential was – 17.6 mV, as determined by dynamic light scattering (Malvern Instruments, Malvern, UK). The encapsulation efficiency was 54.6 %, as detected by high-performance liquid chromatography (HPLC). Based on this encapsulation efficiency, nanoparticles were produced to contain 10 mg/kg of active atorvastatin.

3.4. Motor function recovery and infarct volume assessment

No subjects died after 2 weeks of stroke. Behavioral evaluations were conducted using the NDS and rotarod test before and after treatment in the Sham, Control, LipoStatin, and MagStim + LipoStatin groups to assess motor function recovery after treatment following subacute stroke. After treatment, the NDS in the MagStim + LipoStatin group was

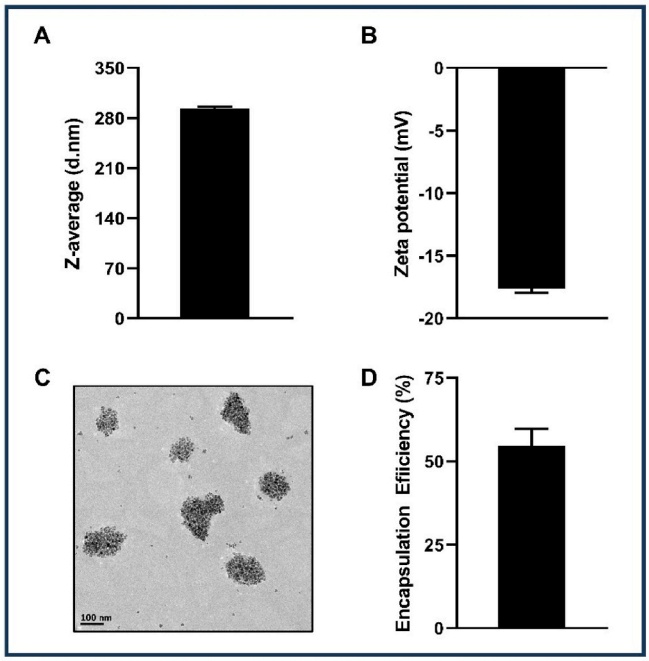

Fig. 4. The quality evaluation results of the LipoStatin. (A) Size and (B) zeta potential of liposomes loaded with atorvastatin calcium. (C) Morphology of the liposomes was assessed using TEM with synomag loaded inside as a negative control. (D) The encapsulation efficiency, which shows the percentage of statin loaded in the liposomes, was determined using high-performance liquid chromatography.

significantly lower than that in the Control group (treatment × time interaction effect, $F_{2,60} = 0.920$, $p = 0.404$; main effect of time, $F_{1,60} = 6.954$, $p = 0.011$; main effect of treatment, $F_{2,60} = 2.308$, $p = 0.108$; two-way ANOVA for repeated measures; $p = 0.010$ compared to the Control group, Tukey's post hoc analysis, Fig. 5A). The rotarod tests assess the coordination, balance, and endurance of an animal after focal ischemic injury and during post-treatment recovery [25]. Fig. 5B shows the recovery improvement rate in the time to fall on the rotarod test before and after treatment in each group. No significant differences in the time to fall were noted among the three experimental groups before treatment. However, the LipoStatin and MagStim + LipoStatin groups exhibited a longer time to fall compared to Control group after treatment (treatment × time interaction effect, $F_{3,80} = 3.219$, $p = 0.027$; main effect of time, $F_{1,80} = 10.268$, $p = 0.002$; main effect of treatment, $F_{3,80} = 15.346$, $p < 0.001$; two-way ANOVA for repeated measures; Control vs. LipoStatin: $p = 0.017$, Control vs. MagStim + LipoStatin: $p = 0.001$, Tukey's post hoc analysis). Thus, the MagStim + LipoStatin group demonstrated better motor function compared to the Control group.

TTC staining was performed to assess the infarction volume in each group. The infarct volume in the group of ischemic rats treated with MagStim + LipoStatin significantly decreased compared to the Control group ($p = 0.004$, Kruskal–Wallis test with Dunn's post hoc test, Fig. 5). Moreover, the infarct volume significantly decreased in the MagStim + LipoStatin group compared to the LipoStatin group ($p = 0.016$).

T2-weighted MR imaging of the rat brain after MCAO induction clearly showed an ischemic region in the control, LipoStatin, and MagStim + LipoStatin groups before therapy. The infarction volumes were measured on T2-weighted MR images before and after treatment. The infarction volume was reduced in the MagStim + LipoStatin group compared to control and LipoStatin groups after treatment (treatment × time interaction effect, $F_{2,15} = 0.895$, $p = 0.429$; main effect of time, $F_{1,15} = 9.129$, $p = 0.009$; main effect of treatment, $F_{2,15} = 3.244$, $p = 0.067$; two-way ANOVA for repeated measures; Control vs. MagStim + LipoStatin: $p = 0.049$, LipoStatin vs. MagStim + LipoStatin: $p = 0.155$, Dunnett's post hoc analysis, Fig. 5).

3.5. Immunoblot analysis for tight junction proteins

We assessed the levels of claudin-5, occludin, ZO-1, and JAM-A to explore the impact of MagStim + LipoStatin on the concentration of tight junction proteins (Fig. 6). Furthermore, we investigated caveolin-1 levels in association with tight junction proteins since Cav-1 acts as a key regulator of BBB permeability. Additionally, we examined the upregulation of MMP-9, which increases BBB permeability [26–29]. The level of tight junction proteins was elevated in the MagStim + LipoStatin group compared to the Control group, indicating improved preservation of BBB integrity through endothelial function restoration (ZO-1: $p < 0.0001$, JAM-A: $p = 0.003$, ANOVA with Dunnett's post hoc analysis; Cav-1: $p < 0.0001$, ANOVA with Tukey's post hoc analysis; Occludin: $p = 0.004$, Claudin-5: $p = 0.004$, Kruskal–Wallis test with Dunn's post hoc analysis). Regarding BBB permeability, the treatment combining MagStim and LipoStatin significantly upregulated the concentration of tight junction proteins ZO-1 and Cav-1 compared with LipoStatin alone in MCAO rats (ZO-1: $p = 0.011$; Cav-1: $p < 0.0001$). The upper band of MMP-9, seen at around 92 kDa, is the precursor form (inactive Pro-MMP-9), and the lower band, seen at around 82 kDa, is the active form [30,31]. The level of the active form of MMP-9, establishing a connection with excitotoxicity and BBB breakdown, decreased significantly in the MagStim + LipoStatin group compared to the Control group ($p = 0.009$, ANOVA with Dunnett's post hoc analysis) [31].

3.6. Assessment of inflammation and neurorestoration markers

MagStim + LipoStatin treatment significantly reduced the protein levels of inflammatory markers of IL-6, TNF-α, and Iba1 compared to the Control and LipoStatin groups in Western blotting (IL-6, TNFα, and Iba1: $p < 0.05$, ANOVA with Tukey's post hoc analysis, Fig. 7A–E). The expression of proinflammatory and restoration factors was analyzed to quantify gene expression after therapy (Fig. 7F–M). The expression of inflammatory cytokines and chemokines, including IL-1β, IL-6, TNF-α, MCP-1, and Iba1, in the MagStim + LipoStatin group decreased compared to the Control group after treatment (IL-1β: $p = 0.825$, IL-6: $p = 0.058$, TNFα: $p = 0.782$, MCP-1: $p = 0.512$, ANOVA with Dunnett's post hoc analysis; Iba1: $p = 0.337$, Kruskal–Wallis test with Dunn's post hoc analysis), although without statistical significance. MagStim + LipoStatin treatment also significantly reduced TNF-α expression compared to the LipoStatin group ($p = 0.020$). The expression of eNOS, which produces vasodilatory nitric oxide, was significantly enhanced in the MagStim + LipoStatin group compared to the Control group ($p = 0.037$, Kruskal–Wallis test with Dunn's post hoc analysis) [32]. Therefore, MagStim, alongside LipoStatin, can be delivered to the ischemic brain region, activating eNOS to promote vasodilation and reduce infarct volume. Additionally, markers of neurorestoration, such as SOX2 and Nestin, further increased in the MagStim + LipoStatin group compared to the Control group, although without statistical significance (SOX2: p = 0.569, Nestin: p = 0.490, ANOVA with Tukey's post hoc analysis, Fig. 7).

3.7. Immunofluorescence for apoptosis and regeneration

We examined CC3/NeuN-positive cells to assess the progression of cell apoptosis in the boundary area of cerebral ischemia (Fig. 8). The number of CC3/NeuN-positive cells markedly increased in the Control group compared to the Sham group ($p < 0.0001$, ANOVA with Tukey's post hoc analysis). However, CC3/NeuN-positive cells significantly decreased in the MagStim + LipoStatin group compared to the Control group ($p < 0.0001$). We evaluated BrdU-positive cells in the mildly damaged frontal cortex to elucidate endogenous regeneration along the boundary region of the cerebral ischemia adjacent to the subventricular zone in the frontal cortex. The number of BrdU/NeuN- and BrdU/DCX-

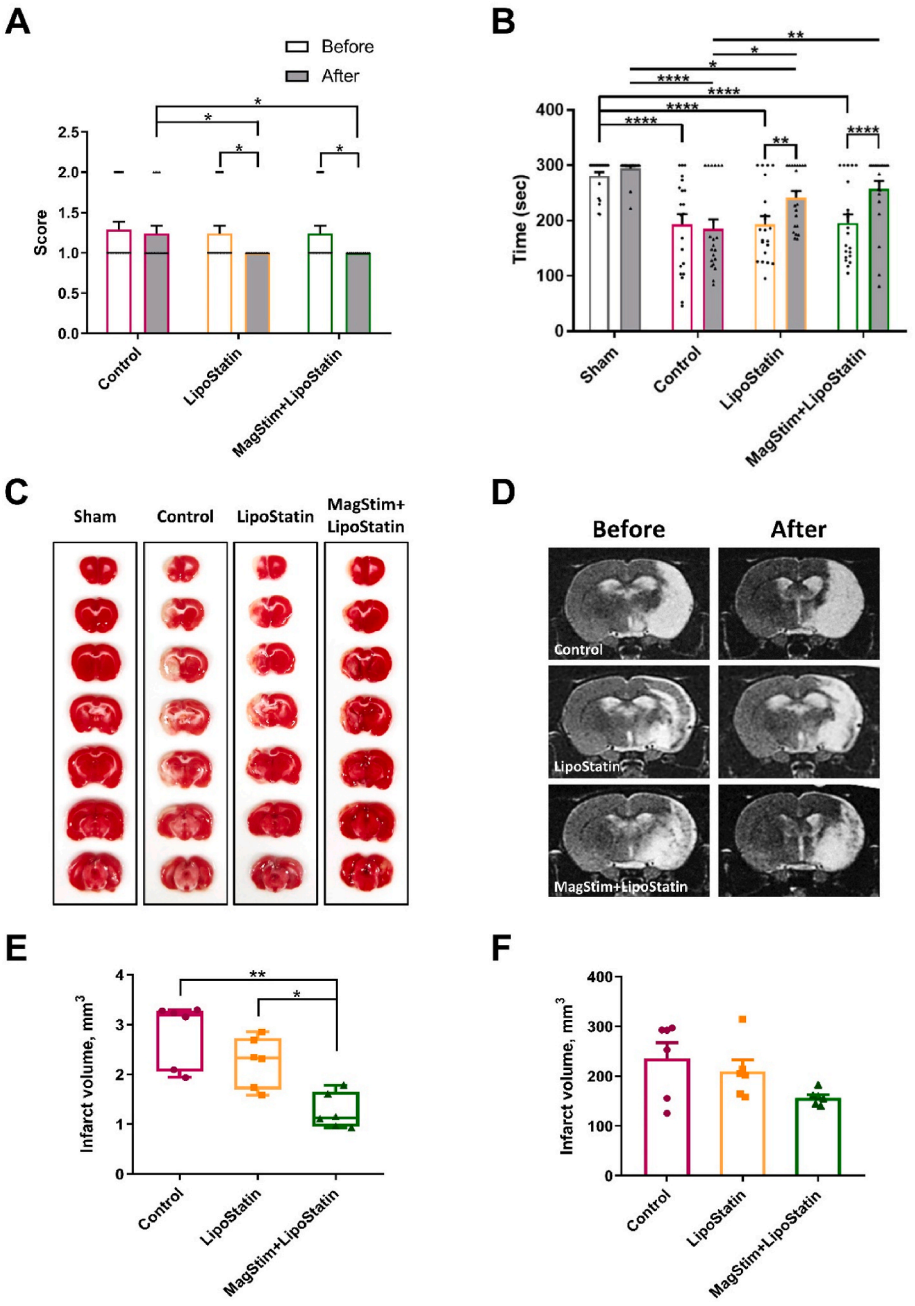

Fig. 5. The MagStim + LipoStatin group showed improved motor function along with a significant reduction in infarct volume. Motor function change was assessed to compare the performance of each group before and after treatment. (A) Neurological deficit score. The data were analyzed by repeated measures ANOVA, n = 21. (B) The improvement rate in the rotarod test before and after treatment was compared among each group. The data were analyzed by repeated measures ANOVA, n = 21. All data are presented as mean ± SEM. *: $p < 0.05$, **: $p < 0.01$. (C) 2 % 2,3,5-triphenyltetrazolium chloride staining of ischemic infarct regions. (D) T2-weighted MR imaging of the rat brain before (2 weeks after stroke) and after treatment (3 weeks after stroke). (E, F) Quantitative analysis results for the extent of infarct volume after treatment. The average volume of the regions of interest showed significant differences among the three groups (n = 6 in each group). (E) Data are presented as the median with interquartile range indicating min to max whiskers of box plots and analyzed using the Kruskal–Wallis test followed by Dunn's post hoc analysis. (F) Data are presented as the mean ± SEM and analyzed by repeated measures ANOVA with Dunnett's post hoc test. *: $p < 0.05$, **: $p < 0.01$.

positive cells was scarcely detected in the Control group. Conversely, BrdU/NeuN- and BrdU/DCX-positive cells were significantly abundant within the penumbra in the MagStim + LipoStatin group compared with the Control and LipoStatin groups (BrdU/NeuN: $p < 0.0001$ compared to the Control group, $p < 0.0001$ compared to the LipoStatin group, ANOVA with Tukey's post hoc analysis; BrdU/DCX: $p < 0.0001$ compared to the Control group, $p < 0.0001$ compared to the LipoStatin group, ANOVA with Dunnett's post hoc analysis, Fig. 8).

4. Discussion

Our results demonstrate that combining MagStim to cross the BBB and LipoStatin in subacute MCAO rats is significantly more effective than saline or LipoStatin treatment alone. By utilizing MagStim to open the BBB and administering LipoStatin, the mechanisms underlying the improvement of motor deficit and metabolic dysfunction include stabilizing the BBB, enhancing endothelial function, reducing neuroinflammation, and promoting neurogenesis. Hence, using MagStim and LipoStatin in combination could serve as a promising targeted therapy to

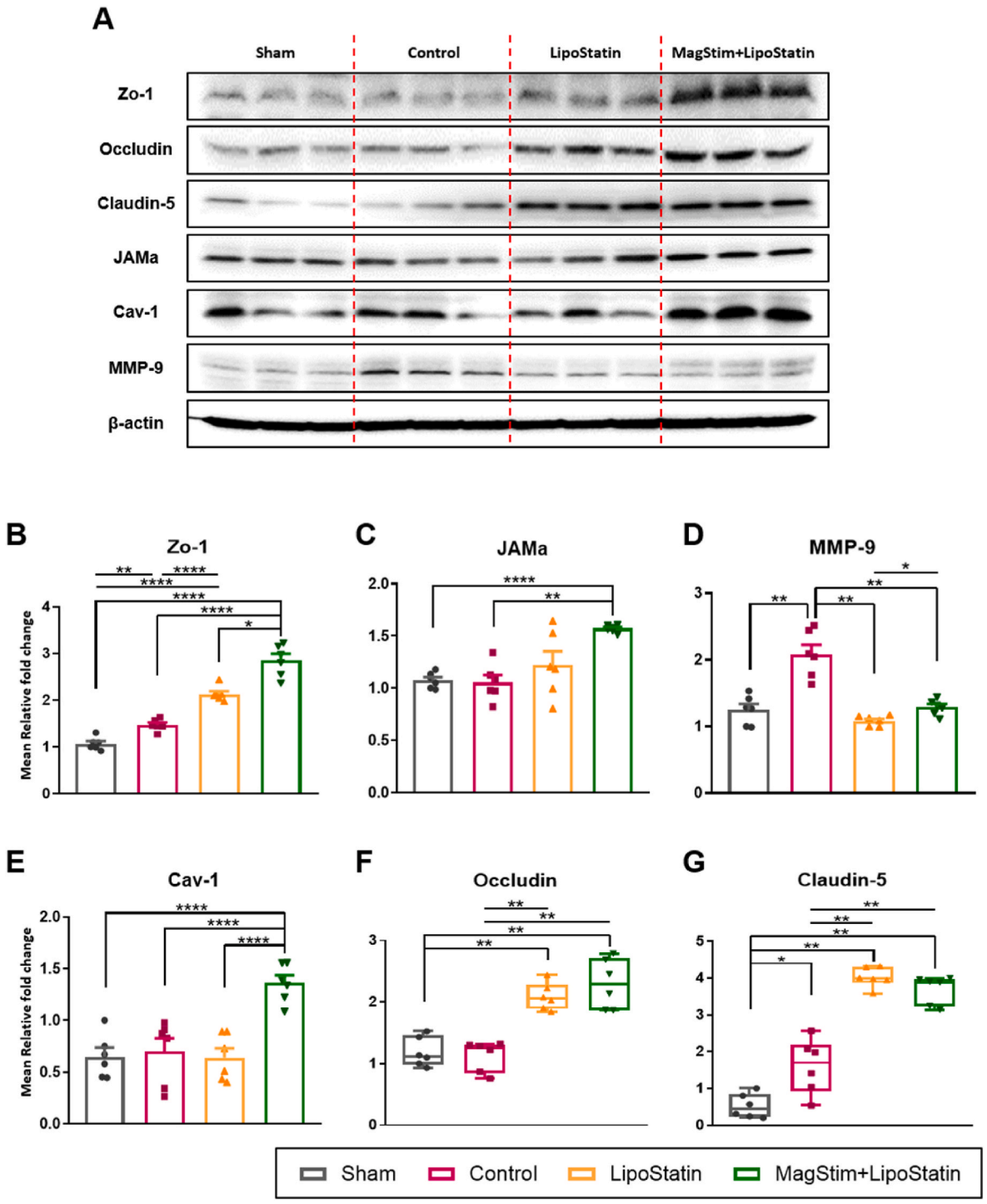

Fig. 6. Evaluation of protein level in ischemic rats after treatment. (A) Protein concentration analyzed by Western blotting: (B) ZO-1, (C) JAM-A, (D) active form of MMP-9 (82 kDa), (E) Cav-1, (F) Occludin, and (G) Claudin-5. Values are normalized to β-actin (n = 6 in each group). (B–D) Data are presented as the mean ± SEM and analyzed by ANOVA with Welch's correction. (E) Data were analyzed by ANOVA with Tukey's post hoc test. (F, G) Data are presented as the median with interquartile range indicating min to max whiskers of box plots and analyzed using the Kruskal–Wallis test. *: $p < 0.05$, **: $p < 0.01$, ***: $p < 0.001$, ****: $p < 0.0001$.

improve functional outcome for patients with subacute stroke, who have no specific treatment option other than secondary prevention and rehabilitation [7]. Our results suggest that the proposed treatment strategy of targeted delivery of a potentially neuroprotective agent to the lesion site using focused MagStim in the subacute period can be effective and safe in a real-world clinical setting after reperfusion is achieved through EVT, the most recommended standard treatment for acute stroke patients with LVO [33].

Our study used IVIS® imaging to assess the increase in BBB permeability and its disruption over time after MCAO. We observed that BBB breakdown peaked by 3 days after ischemia-reperfusion injury and then decreased from day 7. On day 14, it was comparable to that in the non-stroke group (sham group). These results suggest that potential neuroprotective agents can reach the stroke lesion without a specific drug

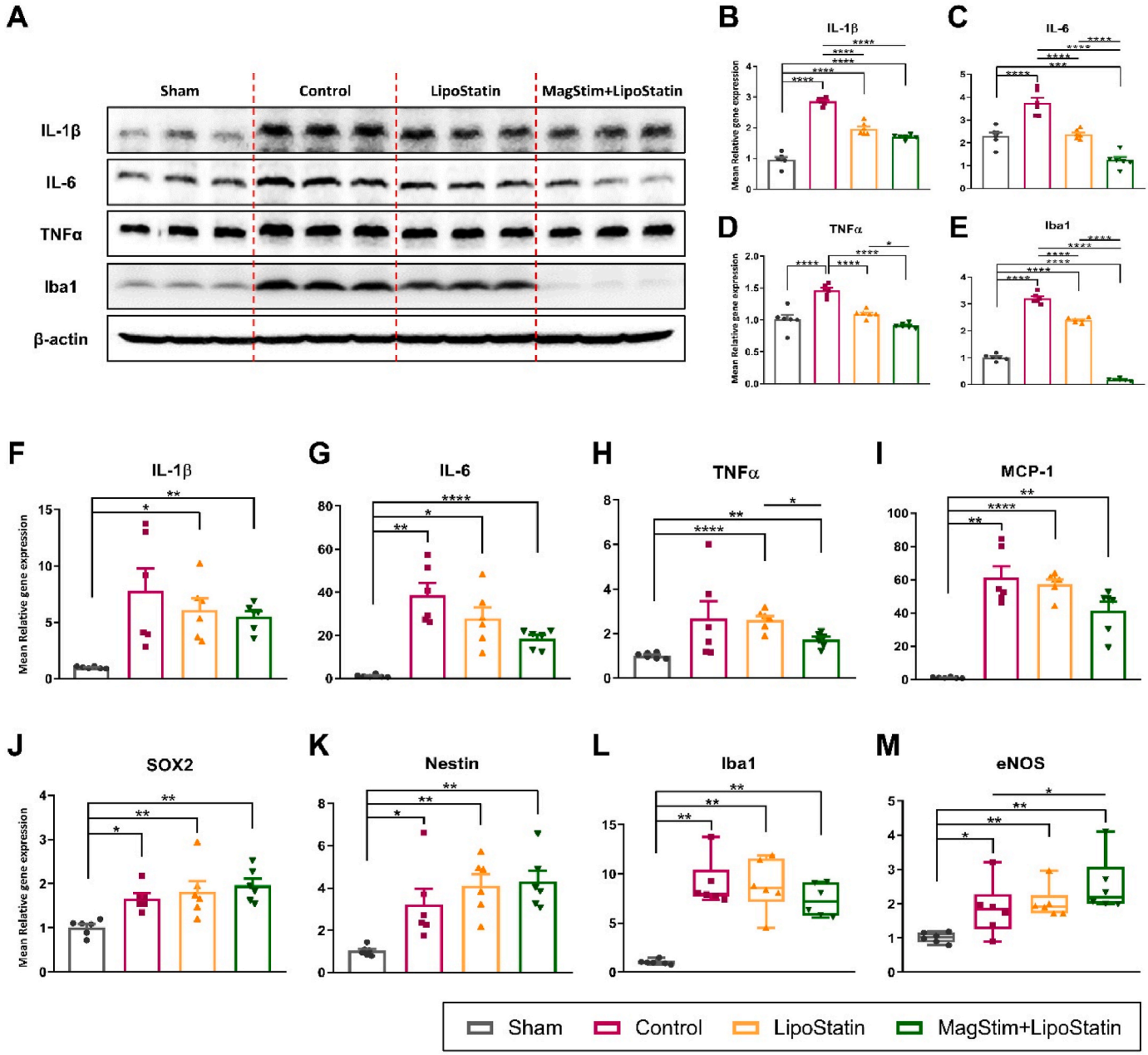

Fig. 7. Inflammation markers were evaluated at the mRNA and protein levels, while neurorestoration markers were analyzed at the mRNA level after treatment. (A) Protein level analyzed by Western blotting: (B) IL-1β, (C) IL-6, (D) TNFα and (E) Iba1; mRNA expression level analyzed by RT-PCR: (F) IL-1β, (G) IL-6, (H) TNFα, (I) MCP-1, (J) SOX2, (K) Nestin, (L) Iba1, and (M) eNOS. (F–I) Data are presented as the mean ± SEM and analyzed by ANOVA with Welch's correction. (B-E, J, K) Data were analyzed by ANOVA with Tukey's post hoc test. (L, M) Data are presented as the median with interquartile range indicating min to max whiskers of box plots and analyzed using the Kruskal–Wallis test. n = 6 in each group. *: $p < 0.05$, **: $p < 0.01$, ***: $p < 0.001$, ****: $p < 0.0001$.

delivery strategy within 14 days after stroke, as BBB damage is present and cerebral vessels are recanalized, and that attempts to open the BBB are risky. However, beyond 14 days after stroke, a treatment strategy that crosses the BBB is necessary for targeted drug delivery. Therefore, to safely address the unmet needs of neuroprotective treatment in subacute stroke following acute reperfusion therapy, we utilized MagStim to increase the efficacy of neuroprotective treatment two weeks after stroke by allowing LipoStatin to cross the BBB and accumulate at the injury site. Current guidelines recommend initiating oral anticoagulant therapy at ≥12–14 days of stroke onset after excluding hemorrhagic transformation, considering the risk of intracerebral hemorrhage, in patients with severe stroke [5,34]. Our treatment schedule is consistent with the treatment timeline currently used in clinical practice. Our results suggest that targeted delivery of drugs with potential neuroprotective effects to the site of ischemic injury using MagStim can further enhance the efficacy of drug therapy safely. Accordingly, this treatment strategy may be a groundbreaking new treatment strategy in the subacute and chronic phases of ischemic stroke.

Our results also demonstrate that theragnostic via magnetic stimulation and imaging could open a new horizon for overcoming neurological diseases. We demonstrated via MPI that the MagStim was indeed effective for targeted drug delivery. Up to 72 h after MagStim, in MPI, nanoparticles crossed the BBB and accumulated within the target area. These results highlight two key aspects of theragnostic: the ability of MagStim to facilitate BBB opening and deliver targeted drugs and the monitoring capability of MPI based on the same technology. Therefore,

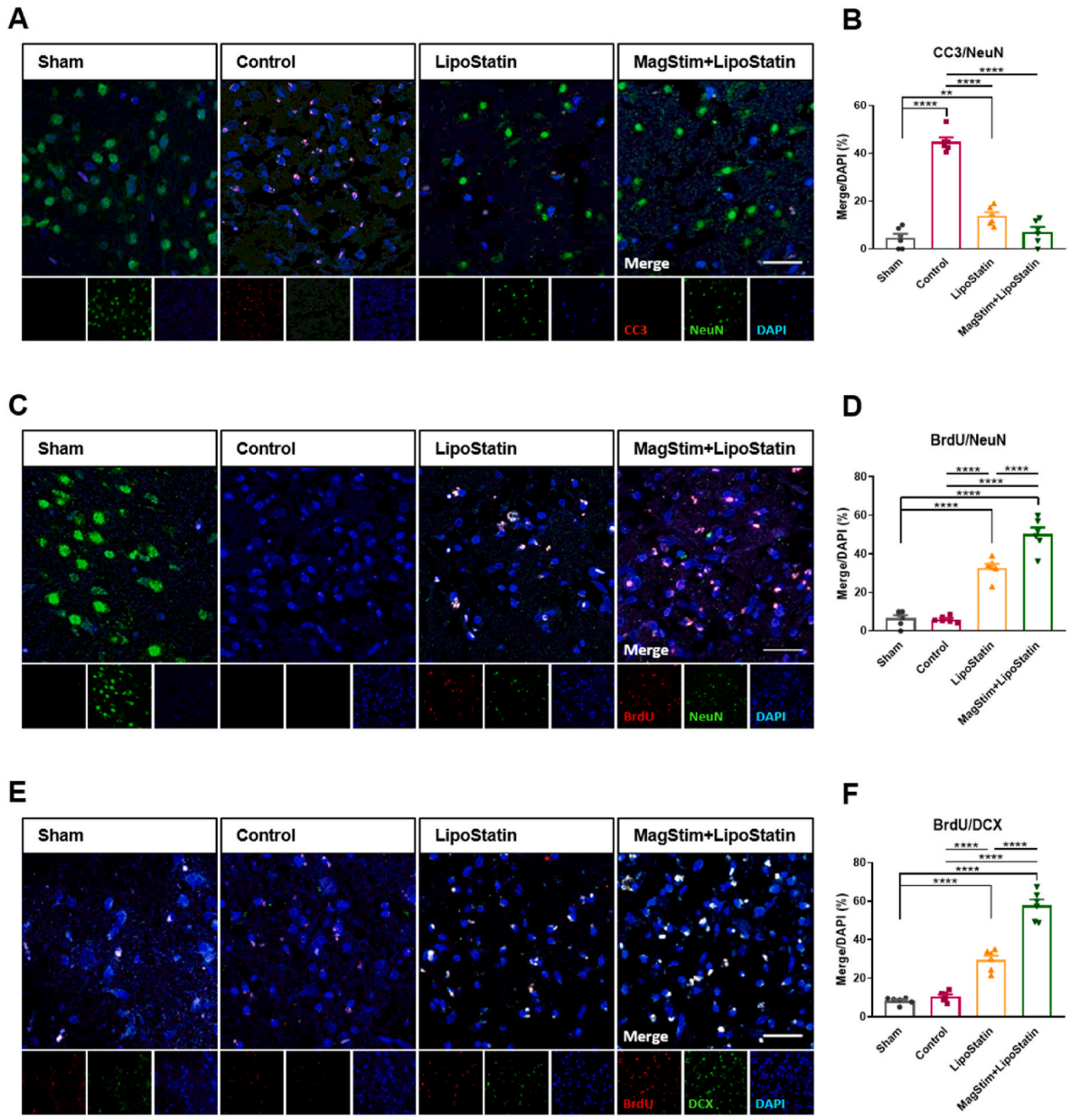

Fig. 8. Confocal images of the ischemic penumbra in the frontal cortex. (A) Images stained for cleaved caspase-3 (CC3; red) and NeuN (green), (C) BrdU (red) and NeuN (green), and (E) BrdU (red) and doublecortin (DCX; green). (B–F) Quantitative analysis of the percentage of CC3 and NeuN colocalization, BrdU and NeuN colocalization, and BrdU and DCX colocalization. CC3/NeuN and BrdU/NeuN graphs were analyzed by ANOVA with Tukey's post hoc test. The BrdU/DCX graph was analyzed by ANOVA with Welch's correction. All data are presented as mean ± SEM (n = 6 in each group; scale bar of 50 μm; 200x magnification). **: $p < 0.01$, ****: $p < 0.0001$.

theragnostic via magnetic stimulation and imaging could be a powerful, noninvasive, and valuable new approach that provides qualitative insights, such as particle localization and residual visualization, and quantitative data, including accurate estimates of particle mass and distribution, in various neurological diseases.

LipoStatin therapy may aid in restoring functional activity by stabilizing the BBB, reducing apoptosis, and enhancing neurogenesis. While ischemia causes immediate cell death, cells in the penumbra, the surrounding area of the ischemic core, sustain potentially reversible injury [35]. Multiple therapeutic approaches have been explored to address abnormal brain activity after ischemic stroke. Furthermore, prior research indicated promising neuroprotective strategies targeting the penumbra area around the ischemic core [3,36,37]. During ischemic injury, the active form of MMP-9 level increases, leading to the degradation of tight junction proteins and BBB disruption [38]. Our results demonstrate that LipoStatin inhibits MMP-9 activity and increases the level of tight junction proteins, stabilizing BBB disruption. Additionally, statins are recognized for their anti-inflammatory and protective effects in ischemic stroke and are believed to modulate microglial activity [39]. Our findings suggest that stabilizing BBB integrity and neuroinflammation with LipoStatin might mitigate cell death during the post-ischemic stroke phase within the peri-infarct region, enhancing motor recovery.

Our results further suggest that MagStim + LipoStatin, opening the BBB and delivering drugs to the target area, provides superior neuroprotective effects over LipoStatin therapy alone. LipoStatin treatment alone may not be effective two weeks after ischemic stroke when the BBB has already stabilized to a certain extent. MagStim + LipoStatin treatment significantly decreased infarct volume compared to LipoStatin therapy alone. Additionally, MagStim + LipoStatin treatment

significantly recovered the level of tight junction proteins and BBB regulatory protein caveolin-1 compared to the LipoStatin group. Moreover, TNF-α, a representative inflammatory cytokine, was considerably lower in the MagStim + LipoStatin group than in the LipoStatin group. MagStim + LipoStatin therapy significantly promoted neurogenesis in the frontal cortex adjacent to the subventricular zone in the ischemic penumbra compared to LipoStatin alone. No subjects died or neurologically deteriorated after MagStim, reaffirming the safety of MagStim. These results were likely obtained due to the improved precise targeting and accumulation of LipoStatin while overcoming the BBB safely by MagStim.

After cerebral ischemia, the brain undergoes molecular changes, including eNOS alterations, which result in changes in endothelial function and vasodilation. Studies suggested that statins confer brain protection against stroke through eNOS, as evidenced by the absence of neuroprotective effects and blood flow regulation in rats lacking eNOS. These findings underscore the significance of enhancing eNOS activity in safeguarding the brain against ischemic injury [40]. As a response to ischemia, eNOS is upregulated to protect the brain against brain damage over time after ischemic stroke. In the MagStim + LipoStatin group, the expression of eNOS, which produces vasodilatory nitric oxide, was enhanced compared to the Control group, while there was no difference between the Control and LipoStatin groups. Therefore, MagStim + LipoStatin can improve endothelial function and vasodilation by upregulating eNOS mRNA expression [41].

Our approach is an innovative, safe drug delivery for targeting deep brain regions without surgery. Our technology for target drug delivery can be applied to all brain regions, including deep brain regions, in a non-invasive manner. Conventional ultrasound and transcranial magnetic stimulation (TMS) have penetration limitations for bone or cavities [42,43]. Therefore, our strategy using MagStim, which can target deep areas while retaining the advantages of conventional TMS and ultrasound, could be a viable approach to reaching usually inaccessible areas. Our results are the first to demonstrate that delivering neuroprotective agents by opening the BBB via MagStim to the targeted ischemic lesions can be effective. Our novel therapeutic strategy may open up new avenues for future research and potential clinical applications for not only ischemic stroke but also many other neurological diseases, such as neurodegenerative disorders.

Nevertheless, certain limitations must be addressed before applying our strategy in clinical settings. First, the study was conducted using an animal model, necessitating further investigation to determine the applicability of these findings to human clinical settings. Although nanotechnology has not yet been approved for treating stroke in humans, the number of FDA-approved nanotechnology-based products and clinical trials in humans has recently increased, primarily in cancer treatment [44]. The leading category applied to humans is liposomes [45]. Therefore, LipoStatin may be a promising novel therapeutic strategy for stroke as a neuroprotective agent, having the potential for application in clinical trials and real-world practice. Second, long-term safety studies are crucial, but our research focuses on short-term outcomes. Our study observed results up to 21 days after stroke, limiting conclusions regarding sustained safety. Thus, longitudinal studies are essential to determine whether LipoStatin offers cumulative long-term benefits. Such studies are particularly important for chronic neurodegenerative diseases, for which ongoing management is critical [46]. Therefore, as a next step, we are investigating long-term neuroprotective effects and potential side effects of statin-loaded NPs in neurodegenerative diseases. Third, our study did not include a positive control, such as rtPA or another neuroprotective agent. Furthermore, statins combined with rtPA may have additional synergistic effects; further studies, including a positive control, are needed [47]. Fourth, we did not directly examine the penetration across the BBB and brain distribution of LipoStatin. Therefore, whether the effects of combined MagStim and LipoStatin treatment result from drug delivery or a synergistic effect of MagStim and LipoStatin alone is unclear. Furthermore, we cannot rule out the possibility that the observed effects are due to MagStim alone, and further research is needed to compare the effectiveness of MagStim alone and MagStim + LipoStatin. However, the primary objective of this study was to evaluate the feasibility and therapeutic efficacy of a MagStim-based drug delivery strategy in patients with subacute stroke who received standard acute reperfusion therapy. Since we demonstrated using MPI that targeted drug delivery is possible by opening the BBB using MagStim, targeted drug delivery into the brain with LipoStatin would also be successful. Furthermore, we demonstrated that MR-based monitoring for target drug delivery is feasible. Therefore, our results suggest that MagStim and nanotherapeutic hybrid approaches may be practical new therapeutic approaches and theranostics.

In conclusion, our study demonstrates the beneficial effects of MagStim and the target delivery of LipoStatin in subacute ischemic stroke after acute reperfusion. This study is the first to demonstrate that combining MagStim and LipoStatin treatment can enhance functional activity, endothelial function, and neuroinflammation, while also promoting neurogenesis and stabilizing the BBB with safety, compared to saline or LipoStatin alone. These findings provide additional evidence regarding the beneficial therapeutic effects of MagStim + LipoStatin, which safely delivers LipoStatin by opening the BBB via MagStim to targeted brain lesions. Our results highlight the need for future advancements of promising novel non-invasive therapeutic MagStim and nanotherapeutic hybrid approaches, which may open new eras for targeted drug delivery and therapy in post-stroke patients and other neurological disorders, such as neurodegenerative diseases, to maximize therapeutic efficacy and minimize systemic side effects.

CRediT authorship contribution statement

Ji-Hye Kim: Writing – original draft, Resources, Methodology, Investigation, Formal analysis, Data curation. **Ja-Hae Kim:** Writing – original draft, Validation, Resources, Methodology, Investigation, Funding acquisition, Formal analysis, Data curation, Conceptualization. **Hafiz Ashfaq Ahmad:** Writing – original draft, Visualization, Methodology, Investigation, Data curation. **Hohyeon Kim:** Visualization, Resources, Methodology, Investigation, Conceptualization. **Raveena Nagareddy:** Resources, Methodology, Investigation, Conceptualization. **Kang-Ho Choi:** Writing – review & editing, Writing – original draft, Validation, Supervision, Resources, Project administration, Methodology, Investigation, Funding acquisition, Formal analysis, Data curation, Conceptualization. **Jungwon Yoon:** Writing – review & editing, Supervision, Resources, Investigation, Funding acquisition, Formal analysis, Data curation, Conceptualization. **Yong-Yeon Jeong:** Writing – review & editing, Validation, Supervision, Resources, Methodology, Investigation.

Declaration of competing interest

The authors declare that they have no known competing financial interests or personal relationships that could have appeared to influence the work reported in this paper.

Acknowledgments

This research was supported by a National Research Foundation (NRF) of Korea Grant funded by the Korean Government (NRF-2023R1A2C2006414 and NRF-2020R1A2C1101082).

References

[1] Tsao CW, Aday AW, Almarzooq ZI, et al. Heart disease and stroke Statistics-2022 update: a report from the American heart association. Circulation 2022;145: e153–639.

[2] Li KP, Wu JJ, Zhou ZL, et al. Noninvasive brain stimulation for neurorehabilitation in post-stroke patients. Brain Sci 2023;13.

[3] Edwards DJ, Liu CY, Dunning K, et al. Electric field navigated 1-Hz rTMS for poststroke motor recovery: the E-FIT randomized controlled trial. Stroke 2023;54:2254–64.
[4] Baker KB, Plow EB, Nagel S, et al. Cerebellar deep brain stimulation for chronic post-stroke motor rehabilitation: a phase I trial. Nat Med 2023;29:2366–74.
[5] Powers WJ, Rabinstein AA, Ackerson T, et al. 2018 guidelines for the early management of patients with acute ischemic stroke: a guideline for healthcare professionals from the American heart association/american stroke association. Stroke 2018;49:e46–110.
[6] Goyal M, Menon BK, van Zwam WH, et al. Endovascular thrombectomy after large-vessel ischaemic stroke: a meta-analysis of individual patient data from five randomised trials. Lancet 2016;387:1723–31.
[7] Kleindorfer DO, Towfighi A, Chaturvedi S, et al. 2021 guideline for the prevention of stroke in patients with stroke and transient ischemic attack: a guideline from the American heart association/american stroke association. Stroke 2021;52:e364–467.
[8] Stroke Prevetion by Aggressive Reduction in Cholestrol Levels I, Karam JG, Loney-Hutchinson L, McFarlane SI. High-dose atorvastatin after stroke or transient ischemic attack: the stroke prevention by aggressive reduction in cholesterol levels (SPARCL) investigators. J Cardiometab Syndr 2008;3:68–9.
[9] Naci H, Brugts JJ, Fleurence R, Tsoi B, Toor H, Ades AE. Comparative benefits of statins in the primary and secondary prevention of major coronary events and all-cause mortality: a network meta-analysis of placebo-controlled and active-comparator trials. Eur J Prev Cardiol 2013;20:641–57.
[10] Askarizadeh A, Butler AE, Badiee A, Sahebkar A. Liposomal nanocarriers for statins: a pharmacokinetic and pharmacodynamics appraisal. J Cell Physiol 2019;234:1219–29.
[11] Yuan J, Li L, Yang Q, et al. Targeted treatment of ischemic stroke by bioactive nanoparticle-derived reactive oxygen species responsive and inflammation-resolving nanotherapies. ACS Nano 2021;15:16076–94.
[12] Munshi R, Qadri SM, Zhang Q, Castellanos Rubio I, Del Pino P, Pralle A. Magnetothermal genetic deep brain stimulation of motor behaviors in awake, freely moving mice. eLife 2017;6.
[13] Chen R, Romero G, Christiansen MG, Mohr A, Anikeeva P. Wireless magnetothermal deep brain stimulation. Science 2015;347:1477–80.
[14] Kim H, Kim J, Kim J, Oh S, Choi K, Yoon J. Magnetothermal-based non-invasive focused magnetic stimulation for functional recovery in chronic stroke treatment. Sci Rep 2023;13:4988.
[15] Thomas RG, Kim JH, Kim JH, Yoon J, Choi KH, Jeong YY. Treatment of ischemic stroke by atorvastatin-loaded PEGylated liposome. Transl Stroke Res 2024;15:388–98.
[16] Koh SH, Park Y, Song CW, et al. The effect of PARP inhibitor on ischaemic cell death, its related inflammation and survival signals. Eur J Neurosci 2004;20:1461–72.
[17] Kho AR, Hong DK, Kang BS, et al. The effects of atorvastatin on global cerebral ischemia-induced neuronal death. Int J Mol Sci 2021;22.
[18] Tu Q, Cao H, Zhong W, Ding B, Tang X. Atorvastatin protects against cerebral ischemia/reperfusion injury through anti-inflammatory and antioxidant effects. Neural Regen Res 2014;9:268–75.
[19] Mendieta G, Ben-Aicha S, Gutierrez M, et al. Intravenous statin administration during myocardial infarction compared with oral post-infarct administration. J Am Coll Cardiol 2020;75:1386–402.
[20] Gerhards L, Deser A, Kattnig DR, Matysik J, Solov'yov IA. Weak radiofrequency field effects on biological systems mediated through the radical pair mechanism. Chem Rev 2025.
[21] Boroon MP, Ayani MB, Bazaz SR. Estimation of the optimum number and location of nanoparticle injections and the specific loss power for ideal hyperthermia. J Therm Biol 2018;72:127–36.
[22] Kim JH, Jeong M, Kim H, et al. Focused magnetic stimulation for motor recovery after stroke. Brain Stimul 2024;17:1048–59.
[23] Kiyatkin EA, Sharma HS. Permeability of the blood-brain barrier depends on brain temperature. Neuroscience 2009;161:926–39.
[24] Zhang Z, Chen TY, Kirsch JR, et al. Kappa-opioid receptor selectivity for ischemic neuroprotection with BRL 52537 in rats. Anesth Analg 2003;97:1776–83.
[25] Hamm RJ, Pike BR, O'Dell DM, Lyeth BG, Jenkins LW. The rotarod test: an evaluation of its effectiveness in assessing motor deficits following traumatic brain injury. J Neurotrauma 1994;11:187–96.
[26] Choi KH, Kim HS, Park MS, et al. Regulation of Caveolin-1 expression determines early brain edema after experimental focal cerebral ischemia. Stroke 2016;47:1336–43.
[27] Li Y, Liu B, Zhao T, et al. Comparative study of extracellular vesicles derived from mesenchymal stem cells and brain endothelial cells attenuating blood-brain barrier permeability via regulating Caveolin-1-dependent ZO-1 and Claudin-5 endocytosis in acute ischemic stroke. J Nanobiotechnol 2023;21:70.
[28] Gu Y, Zheng G, Xu M, et al. Caveolin-1 regulates nitric oxide-mediated matrix metalloproteinases activity and blood-brain barrier permeability in focal cerebral ischemia and reperfusion injury. J Neurochem 2012;120:147–56.
[29] Choi KH, Kim HS, Park MS, et al. Overexpression of caveolin-1 attenuates brain edema by inhibiting tight junction degradation. Oncotarget 2016;7:67857–67.
[30] Kucherenko MM, Sang P, Yao J, et al. Elastin stabilization prevents impaired biomechanics in human pulmonary arteries and pulmonary hypertension in rats with left heart disease. Nat Commun 2023;14:4416.
[31] Velasquez M, O'Sullivan C, Brockett R, et al. Characterization of active MMP9 in chronic inflammatory diseases using a novel Anti-MMP9 antibody. Antibodies 2023;12.
[32] Wei G, Dawson VL, Zweier JL. Role of neuronal and endothelial nitric oxide synthase in nitric oxide generation in the brain following cerebral ischemia. Biochim Biophys Acta 1999;1455:23–34.
[33] Ward NS. Neural plasticity and recovery of function. Prog Brain Res 2005;150:527–35.
[34] Steffel J, Collins R, Antz M, et al. European heart rhythm association practical guide on the use of non-vitamin K antagonist oral anticoagulants in patients with atrial fibrillation. Europace 2021;23:1612–76. 2021.
[35] Fifield KE, Vanderluit JL. Rapid degeneration of neurons in the penumbra region following a small, focal ischemic stroke. Eur J Neurosci 2020;52:3196–214.
[36] Bitar L, Uphaus T, Thalman C, et al. Inhibition of the enzyme autotaxin reduces cortical excitability and ameliorates the outcome in stroke. Sci Transl Med 2022;14:eabk0135.
[37] Adhikari Y, Ma CG, Chai Z, Jin X. Preventing development of post-stroke hyperexcitability by optogenetic or pharmacological stimulation of cortical excitatory activity. Neurobiol Dis 2023;184:106233.
[38] Chen H, Guan B, Wang B, et al. Glycyrrhizin prevents hemorrhagic transformation and improves neurological outcome in ischemic stroke with delayed thrombolysis through targeting peroxynitrite-mediated HMGB1 signaling. Transl Stroke Res 2020;11:967–82.
[39] Churchward MA, Todd KG. Statin treatment affects cytokine release and phagocytic activity in primary cultured microglia through two separable mechanisms. Mol Brain 2014;7:85.
[40] Endres M, Laufs U, Huang Z, et al. Stroke protection by 3-hydroxy-3-methylglutaryl (HMG)-CoA reductase inhibitors mediated by endothelial nitric oxide synthase. Proc Natl Acad Sci U S A 1998;95:8880–5.
[41] Kosmidou I, Moore JP, Weber M, Searles CD. Statin treatment and 3' polyadenylation of eNOS mRNA. Arterioscler Thromb Vasc Biol 2007;27:2642–9.
[42] Tufail Y, Matyushov A, Baldwin N, et al. Transcranial pulsed ultrasound stimulates intact brain circuits. Neuron 2010;66:681–94.
[43] Kobayashi Y, Sakai D, Iwashina T, Iwabuchi S, Mochida J. Low-intensity pulsed ultrasound stimulates cell proliferation, proteoglycan synthesis and expression of growth factor-related genes in human nucleus pulposus cell line. Eur Cell Mater 2009;17:15–22.
[44] Toljan K, Ashok A, Labhasetwar V, Hussain MS. Nanotechnology in stroke: new trails with smaller scales. Biomedicines 2023;11.
[45] Namiot ED, Sokolov AV, Chubarev VN, Tarasov VV, Schioth HB. Nanoparticles in clinical trials: analysis of clinical trials, FDA approvals and use for COVID-19 vaccines. Int J Mol Sci 2023;24.
[46] Pires PC, Paiva-Santos AC, Veiga F. Liposome-derived nanosystems for the treatment of behavioral and neurodegenerative diseases: the promise of niosomes, transfersomes, and ethosomes for increased brain drug bioavailability. Pharmaceuticals 2023;16.
[47] Zhang L, Chopp M, Jia L, Cui Y, Lu M, Zhang ZG. Atorvastatin extends the therapeutic window for tPA to 6 h after the onset of embolic stroke in rats. J Cerebr Blood Flow Metabol 2009;29:1816–24.